PHYSICAL REVIEW D **86,** 114509 (2012)

Nucleon scalar and tensor charges from lattice QCD with light Wilson quarks

J. R. Green, J. W. Negele, and A. V. Pochinsky
Center for Theoretical Physics, Massachusetts Institute of Technology, Cambridge, Massachusetts 02139, USA

S. N. Syritsyn
Nuclear Science Division, Lawrence Berkeley National Laboratory, Berkeley, California 94720, USA

M. Engelhardt
Department of Physics, New Mexico State University, Las Cruces, New Mexico 88003, USA

S. Krieg
Bergische Universität Wuppertal, D-42119 Wuppertal, Germany and IAS, Jülich Supercomputing Centre, Forschungszentrum Jülich, D-52425 Jülich, Germany
(Received 28 June 2012; published 20 December 2012)

We present 2 + 1 flavor lattice QCD calculations of the nucleon scalar and tensor charges. Using the BMW clover-improved Wilson action with pion masses between 149 and 356 MeV and three source-sink separations between 0.9 and 1.4 fm, we achieve good control over excited-state contamination and extrapolation to the physical pion mass. As a consistency check, we also present results from calculations using unitary domain wall fermions with pion masses between 297 and 403 MeV, and using domain wall valence quarks and staggered sea quarks with pion masses between 293 and 597 MeV.

DOI: 10.1103/PhysRevD.86.114509 PACS numbers: 12.38.Gc, 12.60.−i, 13.30.Ce, 14.20.Dh

I. INTRODUCTION

A quantitative understanding of the quark structure of hadrons is essential to relate experimentally observed hadronic properties to fundamental processes occurring at the quark level. Thus, lattice QCD can play a crucial role in determining parameters of the Standard Model from experiment and in predicting the experimental effects of interactions beyond the Standard Model.

One example is the search for the effects of new scalar and tensor couplings beyond the familiar weak interactions of the Standard Model in the decay of ultracold neutrons as discussed in detail in Ref. [1]. These couplings would contribute through the matrix elements $\langle p|\bar{u}d|n\rangle$ and $\langle p|\bar{u}\sigma_{\mu\nu}d|n\rangle$. To leading order in the recoil approximation, these matrix elements are proportional to the isovector scalar and tensor charges g_S and g_T of the nucleon. Hence, lattice QCD predictions of these charges are crucial for determining the sensitivity of the decay process to the nonstandard couplings.

Another example concerns the search for an electric dipole moment of the neutron, which constrains the possible values of the CP-violating strong interaction θ angle. The constant of proportionality between the electric dipole moment and θ can be calculated directly using a background electric field [2,3] or from the CP-odd form factor F_3 (cf. Refs. [4,5]). However, it is also instructive to relate the neutron electric dipole moment near the chiral limit at small θ to the CP-violating pion-nucleon coupling constant $\bar{g}_{\pi NN}$, cf. Ref. [6]. This assumes that $|\pi N\rangle$ intermediate states provide the dominant contribution to the dipole moment, which is the case as $m_\pi \to 0$. In turn, $\bar{g}_{\pi NN}$ is proportional to the isovector scalar charge g_S of the nucleon [6], which thus again appears as an important parameter influencing the search for new physics. Given that the physical limit occurs at finite m_π, where there will be corrections to the relation between the electric dipole moment of the neutron and $\bar{g}_{\pi NN}$, a comparison of this approximation to direct evaluations can also provide insight into the importance of these corrections. Another important effect of $\bar{g}_{\pi NN}$ is the fact that it induces CP violation in nuclear forces resulting in strongly enhanced nuclear electric dipole moments in certain cases [7].

These two examples directly motivate the present work in which we calculate the nucleon's isovector charges g_S and g_T. Since the computationally formidable disconnected contributions from couplings to the sea quarks cancel in these isovector charges, we only calculate the connected contributions. Extensive lattice QCD data generated with three different lattice actions at pion masses ranging between 149 and 597 MeV are reported, together with their extrapolations to the physical pion mass.

In addition to the primary motivation described above, our results also contribute to a more detailed understanding of the nucleon sigma term $\sigma_N = \frac{1}{2}(m_u + m_d)\langle N|\bar{u}u + \bar{d}d|N\rangle$, which determines the part of the nucleon mass generated by the light quark degrees of freedom via the spontaneous breaking of chiral symmetry. Whereas we do not have the resources to evaluate the disconnected contributions to σ_N at present, the connected contributions to $\langle N|\bar{u}u|N\rangle$ and $\langle N|\bar{d}d|N\rangle$ can be given separately and are expected to furnish most of the strength of the nucleon sigma term; cf. Refs. [8–10] for recent lattice studies focusing on σ_N. These quantities are also relevant to dark matter searches

based on Higgs-mediated couplings of baryonic to dark matter [11–13]. For example, the neutralino-nucleon scalar cross-section considered in Ref. [11] can be cast as a linear combination of terms proportional to $\langle N|\bar{u}u|N\rangle$ and $\langle N|\bar{d}d|N\rangle$. Thus, again, the scalar charge g_S of the nucleon (including both isoscalar and isovector components) is useful in quantifying searches for these dark matter candidates.

II. LATTICE METHODOLOGY

The full set of lattice ensembles on which we have calculated our observables is listed in Table I. We make use of three different lattice actions.

Our main results are calculated on ensembles at light pion masses, with tree-level clover-improved Wilson fermions coupled to double HEX-smeared gauge fields, as used by the BMW Collaboration [14]. Operators are renormalized nonperturbatively using the Rome-Southampton method. For the scalar charge, we use renormalization factors calculated by the BMW Collaboration [14], and for the tensor charge we performed our own calculation (see Appendix A). These factors are given in Table II.

For comparison and for a consistency check, we also present results on ensembles with two different lattice actions used for earlier nucleon structure calculations. First, we use unitary domain wall (DW) quarks on ensembles generated by the RBC and UKQCD Collaborations [15,16]. Details of our analysis methods are in Ref. [17]. Operators are renormalized nonperturbatively using the Rome-Southampton method. Z_S [16] and, on the coarse ensemble, Z_T [18] were calculated by the RBC Collaboration. On the fine ensembles, we found $Z_T^{\overline{\text{MS}}(2\text{ GeV})} = 0.8168(9)$ (see Appendix A).

TABLE I. Lattice ensembles used for scalar and tensor charge calculations.

Label	a (fm)	$L_x^3 \times L_t$	m_π (MeV)	$m_\pi L_x a$	Number of configurations	Number of measurements
			Wilson clover			
W1	0.09	$32^3 \times 64$	317(2)	4.6	103	824
W2	0.116	$48^3 \times 48$	149(1)	4.2	646	7752
W3	0.116	$32^3 \times 48$	202(1)	3.8	457	5484
W4	0.116	$32^3 \times 96$	253(1)	4.8	202	2424
W5	0.116	$32^3 \times 48$	254(1)	4.8	420	5040
W6	0.116	$24^3 \times 48$	254(1)	3.6	418	10032
W7	0.116	$24^3 \times 48$	303(2)	4.3	128	768
W8	0.116	$24^3 \times 48$	356(2)	5.0	127	762
			Domain wall			
D1	0.084	$32^3 \times 64$	297(5)	4.0	615	4920
D2	0.084	$32^3 \times 64$	355(6)	4.8	882	7056
D3	0.084	$32^3 \times 64$	403(7)	5.5	527	4216
D4	0.114	$24^3 \times 64$	329(5)	4.6	399	3192
			Mixed action			
M1	0.124	$20^3 \times 64$	293(6)	3.7	460	3680
M2	0.124	$28^3 \times 64$	356(7)	6.3	272	2176
M3	0.124	$20^3 \times 64$	356(7)	4.5	628	5024
M4	0.124	$20^3 \times 64$	495(10)	6.2	483	3864
M5	0.124	$20^3 \times 64$	597(12)	7.5	562	4496

TABLE II. $\overline{\text{MS}}$ renormalization factors at $\mu = 2$ GeV for the tensor and scalar charge on the Wilson clover ensembles.

a (fm)	Z_S	Z_T
0.09	1.107(16)(22)	1.011(5)
0.116	1.115(17)(30)	0.9624(62)

Second, our mixed-action scheme [19,20] uses domain wall valence quarks on gauge configurations with Asqtad staggered sea quarks generated by the MILC Collaboration [21]. Renormalization factors are calculated in the same way [22] as those used in previous calculations of nucleon generalized form factors. One-loop perturbation theory is used to calculate the renormalization factors for all quark bilinear operators evaluated at the one-loop coupling constant and $\mu^2 = 1/a^2$. Because HYP smearing suppresses loop integrals, the ratio $Z_{\mathcal{O},\text{pert}}/Z_{A,\text{pert}}$, where $\mathcal{O}$ denotes a general bilinear and A is the axial current, is within a few percent of unity indicating perturbative corrections are already small at the one-loop level for this ratio. The multiplicative wave function renormalization in the fifth dimension appearing in all renormalization factors is included nonperturbatively by using the five-dimensional conserved axial current for domain wall fermions to calculate $Z_{A,\text{nonpert}}$ and calculating $Z_{\mathcal{O}} = (Z_{\mathcal{O},\text{pert}}/Z_{A,\text{pert}}) \cdot Z_{A,\text{nonpert}}$. The relevant matrix elements are [22] $Z_{A,\text{pert}} = 0.964$, $Z_{S,\text{pert}} = 0.971$, and $Z_{T,\text{pert}} = 0.987$, and the result is evolved to $\mu = 2$ GeV.

For the scalar charge, we can alternatively make use of the renormalization group invariant combination $(m_s - m_{ud})g_S$. Dividing by the physical $m_s - m_{ud}$, as measured in $2 + 1$ flavor lattice QCD calculations in the $\overline{\text{MS}}$ scheme at 2 GeV [16,23–27], and multiplying by a ratio of differences of pseudoscalar meson masses to cancel the leading dependence on quark masses, we get

$$g_S^{\overline{\text{MS}}(2\text{ GeV})} \approx \frac{(m_s^{\text{bare}} - m_{ud}^{\text{bare}})g_S^{\text{bare}}}{m_s^{\text{phys}} - m_{ud}^{\text{phys}}} \times \frac{m_{K,\text{phys}}^2 - m_{\pi,\text{phys}}^2}{m_K^2 - m_\pi^2}, \tag{1}$$

where the physical m_K and m_π in the isospin limit are from Ref. [23] and their values on our mixed-action ensembles were computed in an earlier work [28]. On the mixed-action ensembles, this approach yields values of g_S that differ from the perturbatively renormalized values by between 0.4 and 1.3%. Assuming the perturbative renormalization of the tensor charge has similar errors, we use our perturbative approach for both g_S and g_T and conservatively estimate a systematic error due to renormalization of 2%.

We compute nucleon forward matrix elements using the usual ratio-plateau method [17,19]. Beginning with two-point and three-point functions,

TABLE III. Source-sink separations T.

Action	a (fm)	T/a
Mixed	0.124	9
Domain wall	0.084	12
Domain wall	0.114	9
Wilson clover	0.09	10, 13, 16
Wilson clover	0.116	8, 10, 12

$$C_{2\mathrm{pt}}(t,\vec{P}) = \langle N(\vec{p}=\vec{P},t)\bar{N}(\vec{x}=0,0)\rangle, \tag{2}$$

$$C^{\mathcal{O}}_{3\mathrm{pt}}(\tau,T;\vec{P}) = \langle N(\vec{p}=\vec{P},T)\mathcal{O}(\vec{p}=0,\tau)\bar{N}(\vec{x}=0,0)\rangle, \tag{3}$$

where N is our lattice nucleon interpolating operator, we compute their ratio,

$$R^{\mathcal{O}}(\tau,T;\vec{P}) = \frac{C^{\mathcal{O}}_{3\mathrm{pt}}(\tau,T;\vec{P})}{C_{2\mathrm{pt}}(T,\vec{P})}. \tag{4}$$

At sufficiently large τ and $T-\tau$, contributions from excited states are negligible, and the ratio gives us the matrix element $\langle N(\vec{P})|\mathcal{O}|N(\vec{P})\rangle$. In practice, for a fixed source-sink separation T, we take the average over the central two or three points of the plateau as the matrix element. The matrix elements give us the isovector scalar and tensor charges:

$$\langle N(\vec{P})|\bar{u}u - \bar{d}d|N(\vec{P})\rangle = g_S\bar{u}(\vec{P})u(\vec{P}), \tag{5}$$

$$\langle N(\vec{P})|\bar{u}\sigma_{\mu\nu}u - \bar{d}\sigma_{\mu\nu}d|N(\vec{P})\rangle = g_T\bar{u}(\vec{P})\sigma_{\mu\nu}u(\vec{P}). \tag{6}$$

We take the weighted average of results measured with $\vec{P}=0$ and $\vec{P}=\frac{2\pi}{L}(-1,0,0)$. The source-sink separations T that we use are listed in Table III. On the Wilson action ensembles, we perform measurements at three source-sink separations in order to better identify systematic errors from excited-state contamination. However, our main results are presented using the middle separation, with $T \approx 1.16$ fm.

Chiral perturbation theory results for g_A and g_T are summarized in Appendix B.

III. RESULTS

The dependence on source-sink separation for the Wilson-clover data is shown in Fig. 1 for the scalar charge and in Fig. 2 for the tensor charge. Neither observable shows a strong statistically significant dependence on source-sink separation.

The main results for the scalar charge are presented in Fig. 3. There is broad agreement between the different actions, although they are not entirely consistent. In particular, the two mixed-action ensembles at $m_\pi = 356$ MeV have points that lie significantly below the point

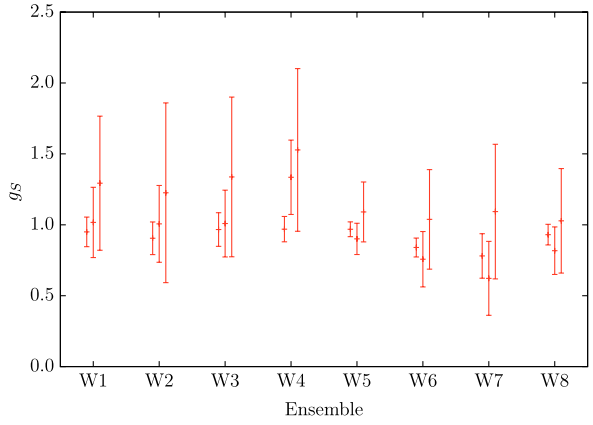

FIG. 1 (color online). Scalar charge measured at three source-sink separations on the Wilson-clover ensembles, as enumerated in Table I.

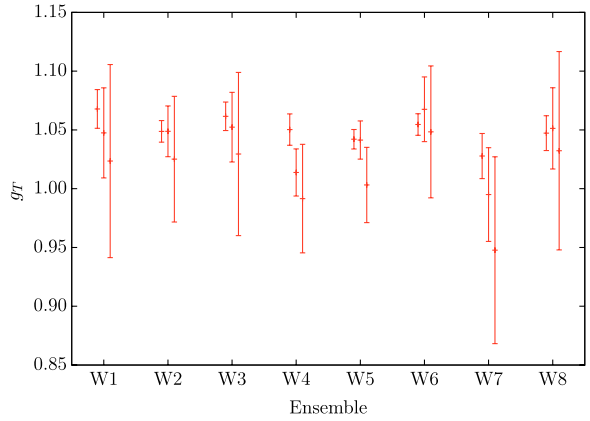

FIG. 2 (color online). Tensor charge measured at three source-sink separations on the Wilson-clover ensembles, as enumerated in Table I.

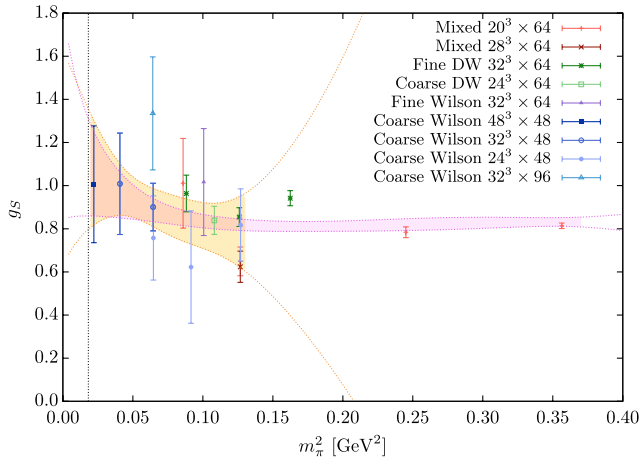

FIG. 3 (color online). g_S versus m_π^2. Error bars are purely statistical and do not include errors in renormalization factors, which are correlated across ensembles with the same action. Two chiral fits are shown: a three-parameter fit to the coarse Wilson-clover ensembles (shaded up to $m_\pi^2 < 0.13$ GeV^2) and a four-parameter fit to all shown ensembles.

for the domain wall ensemble at $m_\pi = 355$ MeV. We estimate the value of the scalar charge at the physical pion mass, 135 MeV, in three ways:

(1) Taking the value from our ensemble with the lowest pion mass, 149 MeV. Including the error in Z_S, this is $g_S = 1.01(27)$.

(2) Performing a three-parameter chiral fit to the set of seven $a = 0.116$ Wilson-clover ensembles. This is a good fit with $\chi^2/\text{dof} = 3.99/4$ and is shown in Fig. 3. Extrapolating to the physical pion mass yields $g_S = 1.08(28)$.

(3) Performing a four-parameter chiral fit to the full set of ensembles. The tension at higher pion masses between the domain wall and the mixed action ensembles is reflected in $\chi^2/\text{dof} = 30.23/13$. Extrapolation yields $g_S = 1.08(23)$.

Our tensor charge results are shown in Fig. 4. Note that the vertical scale is expanded and the error bars are much smaller. Again there is general agreement between different lattice actions. The figure shows some inconsistency between the domain wall and mixed-action ensembles at larger pion masses. However, this is close to the 2% correlated error that we assign to the mixed-action results to account for perturbative renormalization. As with the scalar charge, we estimate the physical value of g_T in three ways:

(1) Using the value from the $m_\pi = 149$ MeV ensemble yields $g_T = 1.049(23)$.

(2) Performing a two-parameter chiral fit to the coarse Wilson-clover ensembles. As with the scalar charge, the fit works well with $\chi^2/\text{dof} = 4.49/5$. However, the fit chooses $\mu^2 = 0$, which removes the chiral log. At the physical pion mass, this gives $g_T = 1.038(11)$.

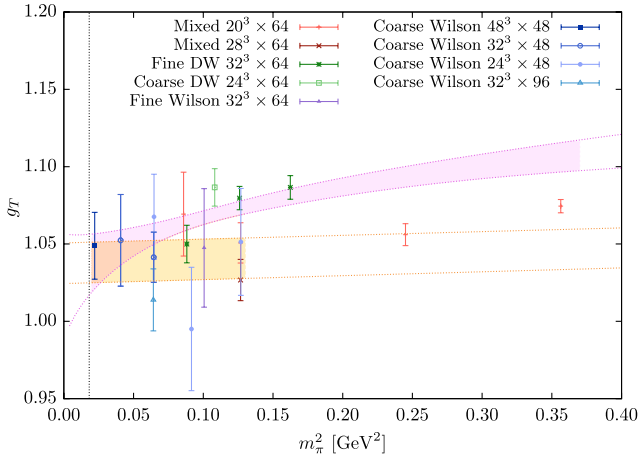

FIG. 4 (color online). g_T versus m_π^2. Error bars are purely statistical and do not include errors in renormalization factors, which are correlated across ensembles with the same action. Two chiral fits are shown: a two-parameter fit to the coarse Wilson-clover ensembles (shaded up to $m_\pi^2 < 0.13\,\text{GeV}^2$) and a three-parameter fit to all shown ensembles.

(3) Performing a three-parameter fit to the full set of ensembles. Because of the correlated error for the mixed-action ensembles, this fit also works well, giving $\chi^2/\text{dof} = 19.69/14$. Extrapolating to the physical pion mass yields $g_T = 1.037(20)$.

IV. SUMMARY AND CONCLUSIONS

Motivated by the facts that contributions of nonstandard scalar and tensor couplings to neutron decay are proportional to isovector g_S and g_T, and that $\bar{g}_{\pi NN}$, which produces parity-violating components of nucleon-nucleon interactions, is proportional to isovector g_S, we have undertaken a comprehensive set of calculations of g_S and g_T using lattice QCD.

Our calculation includes a number of significant advances. We have utilized three sets of ensembles that cover different pion mass regions for which we use the same calculational methodology. The primary data for this analysis were obtained using the smeared Wilson-clover action developed by the BMW Collaboration and include pion masses in the vicinity of 150, 200, 250, 300, and 350 MeV. The 149 MeV pion mass plays a crucial role in our analysis. It is so close to the physical pion mass that it virtually eliminates uncertainty from extrapolation to the physical mass and is well below the lowest mass used in other calculations. Furthermore, given the known strong source-sink separation dependence in some observables such as the momentum fraction, our careful study of 3 separations in Figs. 1 and 2 from 0.93 to 1.39 fm is important in ruling out contributions of excited states near the physical pion mass.

To control systematic effects from finite lattice volume, we have satisfied the standard criterion $m_\pi L_x a > 4$ for nearly all of our ensembles, including the crucial $m_\pi = 149$ MeV ensemble where $m_\pi L_x a = 4.2$ (cf. Table I). In addition, we carried out an explicit test for finite volume effects using the two ensembles W5 and W6 at $m_\pi = 254$ MeV, which are identical except for their lattice volume. Within the statistical accuracy of our calculation, no significant deviations between the results obtained in these two ensembles were found.

Comparison of values of g_S and g_T for the ensembles W1 with lattice spacing $a = 0.09$ fm and W7 with $a = 0.116$ fm at similar values of m_π and $L_x a$, cf. Table I, indicates the absence of a dependence within our statistical errors.

Supplementing the results obtained at the pion mass $m_\pi = 149$ MeV, we performed three- and four-parameter chiral fits to g_S and g_T for the low mass Wilson ensembles, where we expect chiral perturbation theory to be valid. These fits serve as a check on the consistency of the 149 MeV data point and have the potential to reduce the statistical error. The central values of the 149 MeV data points and fits were essentially identical on the scale of the errors, and it turned out that the error in the scalar charge was essentially unchanged while the error on the tensor charge was cut in

half. We regard the chiral fits to the Wilson-clover data as our definitive results for the central values and statistical error. We also estimate the systematic error from excited-state contamination as the average of two absolute differences; those between the central value from the middle source-sink separation on the 149 MeV ensemble and the central values from the other two source-sink separations on that ensemble, i.e., $\frac{1}{2}(|g_X^{T=10a} - g_X^{T=8a}| + |g_X^{T=10a} - g_X^{T=12a}|)$. This yields $g_S = 1.08 \pm 0.28(\text{stat}) \pm 0.16(\text{syst})$ and $g_T = 1.038 \pm 0.011(\text{stat}) \pm 0.012(\text{syst})$. We emphasize that our results do not hinge decisively on chiral perturbation theory. The chiral fits to the data at higher pion masses rather serve to buttress the calculations at $m_\pi = 149$ MeV, which by themselves represent determinations of g_S and g_T with essentially no residual uncertainty due to chiral extrapolation.

The range of pion masses for the Wilson action overlaps the range 297–403 MeV for the domain wall action and the range 293–597 MeV for the mixed action, so simultaneous analysis provides a valuable consistency check of the actions and normalization. In the region of overlap between the Wilson-clover and domain wall calculations, the results agreed well, confirming the underlying consistency of these two calculations including normalization. There is a certain tension between the mixed action and domain wall results at higher pion masses, the origin of which we have not been able to pinpoint; an underestimate of the renormalization uncertainties in the mixed-action case is one possible source. When the error in the normalization is taken into account, the four- and three-parameter chiral fits to g_S and g_T for all three sets of ensembles are consistent with the chiral fits to the low mass Wilson ensembles, as reflected in the close agreement of the error envelopes at the physical pion mass.

Concerning other systematic uncertainties, we have yet to perform extensive low mass Wilson calculations at smaller lattice spacings to extrapolate to the continuum limit and at larger volumes to extrapolate to the infinite volume limit. At the present level of statistics, our comparison of two different lattice volumes at the pion mass $m_\pi = 254$ MeV and two different lattice spacings at $m_\pi \approx 300$ MeV yielded no evidence of significant volume or lattice spacing effects. However, in view of past experience with the well-studied case of the nucleon axial charge g_A, future more statistically accurate calculations may yet necessitate more detailed investigations of a range of volumes and lattice spacings. Comparable calculations of g_A by several groups including our own lie below the experimental value by more than the statistical errors, and it is likewise possible that the aforementioned or other systematic errors in g_S and g_T are still appreciable.

ACKNOWLEDGMENTS

We thank Zoltan Fodor for useful discussions and the Budapest-Marseille-Wuppertal Collaboration for making some of their configurations available to us. This research used resources of the Argonne Leadership Computing Facility at Argonne National Laboratory, which is supported by the Office of Science of the U.S. Department of Energy under Contract No. DE-AC02-06CH11357, resources provided by the New Mexico Computing Applications Center (NMCAC) on Encanto, resources at Forschungszentrum Jülich, and facilities of the USQCD Collaboration, which are funded by the Office of Science of the U.S. Department of Energy. During this research J. R. G., J. W. N., and A. V. P. were supported in part by the U.S. Department of Energy Office of Nuclear Physics under Grant No. DE-FG02-94ER40818, M. E. was supported in part by DOE Grant No. DE-FG02-96ER40965, S. N. S. was supported in part by DOE Contract No. DE-AC02-05CH11231, and S. K. was supported in part by Deutsche Forschungsgemeinschaft through Grant No. SFB-TR 55. The Chroma software suite [33] was used for the mixed action and DWF calculations. The Wilson-clover calculations were performed with Qlua software.

APPENDIX A: NONPERTURBATIVE RENORMALIZATION OF THE TENSOR CHARGE OPERATOR

In this section, we briefly describe the method and present the results of computing the nonperturbative renormalization factors $Z_T^{\overline{\text{MS}}(2\text{ GeV})}$ for the tensor charge g_T, $Z_T^{\overline{\text{MS}}(2\text{ GeV})} g_T^{\text{lat}} = g_T^{\overline{\text{MS}}(2\text{ GeV})}$, for clover-improved Wilson and domain wall fermion ensembles.

Following Ref. [29], we compute amputated lattice Green functions Π_T^{lat} of tensor charge operator and plane wave quarks $q(x) \sim e^{ipx}$, $p^2 = \mu^2$ in the Landau gauge. We then extract the lattice renormalization factor Z_T^{lat} defined as $(Z/Z_q)^{\text{lat}} \Pi^{\text{lat}} = \Pi^{\text{tree}}$, where Π^{tree} is the corresponding tree-level amputated Green function and Z_q is the quark field renormalization. In order to match lattice-regulated and perturbatively renormalized operators, we compute scale-independent (SI) renormalization factors Z_T^{SI}

$$\frac{Z_T^{\text{SI}}}{Z_V} = \left[\left(\frac{Z_T}{Z_V} \right)^{\text{lat}}_{p^2=\mu^2} \cdot \left(\frac{Z_T^{RI'(2\text{ GeV})}}{Z_T^{RI'(\mu)}} \right)^{\text{pert}} \right]_{m_q \to 0, \mu \to 0}, \quad \text{(A1)}$$

where the perturbative operator renormalization is calculated to order $O(\alpha_S^3)$ [30] and Z_V^{lat} is the renormalization of the quark charge operator on the lattice,

$$(Z_V/Z_q)^{\text{lat}} \cdot \langle N(\vec{P}) | u^\dagger u - d^\dagger d | N(\vec{P}) \rangle_{\text{lat}} \doteq 1. \quad \text{(A2)}$$

We extrapolate linearly first in $m_q \to 0$, and then in $\mu^2 \to 0$ in the range $\mu^2 \approx 6 \ldots 15\ \text{GeV}^2$ (see Fig. 5). Finally, we obtain the renormalization factors for converting lattice results into the $\overline{\text{MS}}(2\text{ GeV})$ scheme:

$$Z_T^{\overline{\text{MS}}(2\text{ GeV})} = \left(\frac{Z_T^{\text{SI}}}{Z_V} \right) \cdot Z_V^{\text{lat}} \cdot \left(\frac{Z_T^{\overline{\text{MS}}(2\text{ GeV})}}{Z_T^{RI'(2\text{ GeV})}} \right)^{\text{pert}}. \quad \text{(A3)}$$

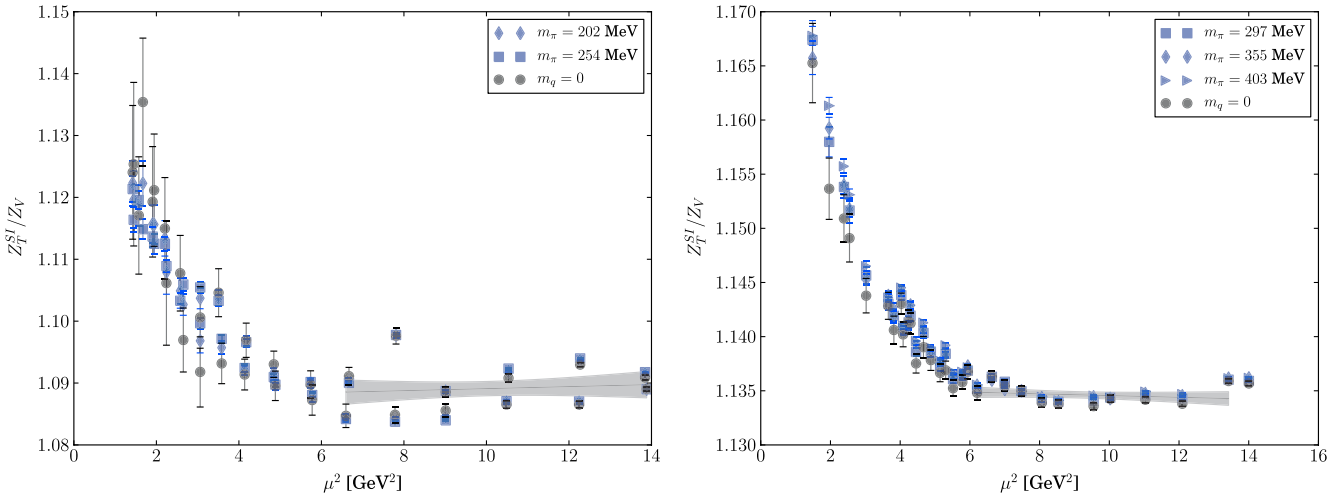

FIG. 5 (color online). Extrapolations of the scale-independent (SI) ratio ($Z_T^{\rm SI}/Z_V^{\rm lat}$) for coarse clover-improved Wilson fermion lattice ensembles (W3, W5) (left) and fine domain wall fermion lattices (D1–D3) (right).

APPENDIX B: CHIRAL PERTURBATION THEORY

For chiral extrapolation of the scalar charge, we make use of the Feynman-Hellmann theorem to obtain

$$g_S \equiv \langle p|\bar{u}u - \bar{d}d|p\rangle = \left(\frac{\partial}{\partial m_u} - \frac{\partial}{\partial m_d}\right)M_p. \quad \text{(B1)}$$

Strong isospin splitting of nucleon masses has been computed in $SU(2)$ heavy baryon chiral perturbation theory, with explicit Δ degrees of freedom, to next-to-next-to-leading order, i.e., to $\mathcal{O}(m_q^2)$ [31]. This leads to the expression

$$\begin{aligned} g_S(m_\pi^2) = 2\alpha_M &- \frac{1}{2(4\pi F_\pi)^2}\Big\{m_\pi^2 \\ &\times\Big[8\Big(g_A^2\alpha_M + g_{\Delta N}^2\Big(\alpha_M + \frac{5}{9}\gamma_M\Big)\Big) \\ &- (b_1^M + b_6^M)\frac{\pi(\sqrt{2}F_\pi)^3}{\lambda}\Big] \\ &+ m_\pi^2\log\Big(\frac{m_\pi^2}{\mu^2}\Big)2\alpha_M(6g_A^2+1) \\ &+ \mathcal{J}(m_\pi,\Delta,\mu)8g_{\Delta N}^2\Big(\alpha_M + \frac{5}{9}\gamma_M\Big)\Big\}, \end{aligned} \quad \text{(B2)}$$

where

$$\begin{aligned} \mathcal{J}(m,\Delta,\mu) = (m^2 - 2\Delta^2)\log\frac{m^2}{\mu^2} \\ + 2\Delta\sqrt{\Delta^2 - m^2}\log\Big(\frac{\Delta - \sqrt{\Delta^2 - m^2 + i\epsilon}}{\Delta + \sqrt{\Delta^2 - m^2 + i\epsilon}}\Big) \\ + 2\Delta^2\log\frac{4\Delta^2}{\mu^2}. \end{aligned} \quad \text{(B3)}$$

Here F_π, g_A, and Δ are the pion decay constant, the nucleon axial charge, and the $\Delta(1232)$-nucleon mass splitting, respectively, in the $SU(2)$ chiral limit. The convention used here is that the physical value of F_π is approximately 92 MeV. We fix these three parameters to values used for chiral extrapolation in a previous nucleon structure calculation [19],

$$F_\pi = 86.2\,\text{MeV}, \quad g_A = 1.2, \quad \Delta = 0.2711\,\text{GeV}, \quad \text{(B4)}$$

leaving three independent parameters to which we fit our $g_S(m_\pi^2)$ data. If we fix only Δ, then the resulting fit has four independent parameters.

Chiral extrapolation formulas for the tensor charge are given in Ref. [32]. Full formulas including Δ loops are given via a number of integrals, and then it is shown that these are approximated well by an expression that includes only the leading nonanalytic term. Also including terms that connect to the heavy quark limit, chiral extrapolation for the tensor charge gives:

$$\begin{aligned} g_T(m_\pi^2) = \delta a\Big(1 + \delta c_{\rm LNA} m_\pi^2\log\frac{m_\pi^2}{m_\pi^2 + \mu^2}\Big) \\ + \delta b\frac{m_\pi^2}{m_\pi^2 + m_b^2}, \end{aligned} \quad \text{(B5)}$$

where from the heavy quark limit

$$\delta b = \frac{5}{3} - \delta a(1 - \mu^2\delta c_{\rm LNA}), \quad \text{(B6)}$$

and the coefficient of the log term,

$$\delta c_{\rm LNA} = \frac{-1}{2(4\pi F_\pi)^2}\Big[\Big(2 - \frac{4}{9}\frac{g_{\pi N\Delta}^2}{g_{\pi NN}^2}\Big)g_A^2 + \frac{1}{2}\Big]. \quad \text{(B7)}$$

Fixing $m_b = 5$ GeV as in Ref. [32] yields a fit with three independent parameters. In addition, fixing g_A and F_π as for the scalar charge, and $\frac{g_{\pi N\Delta}}{g_{\pi NN}} = 1.85$, reduces the number of independent parameters to two.

APPENDIX C: TABLE OF RESULTS

Table IV contains the scalar and tensor data from our full set of ensembles.

TABLE IV. Full set of results for the scalar and tensor charges. The isovector data are renormalized in the $\overline{\text{MS}}$ scheme at $\mu = 2$ GeV, whereas the $u + d$ data contain only the connected contribution and are not renormalized. Wilson data, W1–W8, are from the middle source-sink separation.

		Scalar		Tensor	
Ensemble	m_π (MeV)	$u - d$	$u + d$	$u - d$	$u + d$
W1	317(2)	1.017(248)	5.618(388)	1.047(38)	0.700(46)
W2	149(1)	1.006(271)	10.127(1.501)	1.049(22)	0.652(33)
W3	202(1)	1.009(235)	6.632(620)	1.052(30)	0.622(46)
W4	253(1)	1.335(262)	7.808(906)	1.014(20)	0.598(55)
W5	254(1)	0.901(110)	6.027(251)	1.041(16)	0.676(22)
W6	254(1)	0.757(195)	5.241(935)	1.068(28)	0.668(33)
W7	303(2)	0.622(260)	4.923(395)	0.995(40)	0.656(63)
W8	356(2)	0.817(168)	5.128(268)	1.051(35)	0.691(46)
D1	297(5)	0.964(85)	8.933(195)	1.050(12)	0.779(19)
D2	355(6)	0.854(43)	8.114(102)	1.080(8)	0.807(11)
D3	403(7)	0.941(35)	7.903(81)	1.087(8)	0.802(11)
D4	329(5)	0.839(65)	8.193(153)	1.087(12)	0.827(18)
M1	293(6)	1.012(208)	6.624(278)	1.069(27)	0.543(34)
M2	356(7)	0.624(73)	4.912(89)	1.027(13)	0.546(14)
M3	356(7)	0.648(67)	4.944(97)	1.051(13)	0.557(14)
M4	495(10)	0.787(25)	3.908(35)	1.056(7)	0.566(7)
M5	597(12)	0.814(13)	3.495(17)	1.074(4)	0.574(4)

[1] T. Bhattacharya, V. Cirigliano, S. D. Cohen, A. Filipuzzi, M. Gonzalez-Alonso, M. Graesser, R. Gupta, and H.-W. Lin, Phys. Rev. D **85**, 054512 (2012).

[2] E. Shintani, S. Aoki, N. Ishizuka, K. Kanaya, Y. Kikukawa, Y. Kuramashi, M. Okawa, A. Ukawa, and T. Yoshié, Phys. Rev. D **75**, 034507 (2007).

[3] E. Shintani, S. Aoki, and Y. Kuramashi, Phys. Rev. D **78**, 014503 (2008).

[4] R. Horsley, T. Izubuchi, Y. Nakamura, D. Pleiter, P. E. L. Rakow, G. Schierholz, and J. Zanotti, arXiv:0808.1428.

[5] K.-F. Liu, Mod. Phys. Lett. A **24**, 1971 (2009).

[6] R. Crewther, P. Di Vecchia, G. Veneziano, and E. Witten, Phys. Lett. **88B**, 123 (1979).

[7] W. Haxton and E. Henley, Phys. Rev. Lett. **51**, 1937 (1983).

[8] H. Ohki, H. Fukaya, S. Hashimoto, T. Kaneko, H. Matsufuru, J. Noaki, T. Onogi, E. Shintani, and N. Yamada, Phys. Rev. D **78**, 054502 (2008).

[9] S. Dürr, Z. Fodor, T. Hemmert, C. Hoelbling, J. Frison *et al.*, Phys. Rev. D **85**, 014509 (2012).

[10] R. Horsley, Y. Nakamura, H. Perlt, D. Pleiter, P. Rakow, G. Schierholz, A. Schiller, H. Stüben, F. Winter, and J. Zanotti, Phys. Rev. D **85**, 034506 (2012).

[11] A. Bottino, F. Donato, N. Fornengo, and S. Scopel, Astropart. Phys. **18**, 205 (2002).

[12] J. R. Ellis, K. A. Olive, Y. Santoso, and V. C. Spanos, Phys. Rev. D **71**, 095007 (2005).

[13] *Particle Dark Matter: Observations, Models and Searches*, edited by G. Bertone (Cambridge University Press, Cambridge, England, 2010).

[14] S. Dürr, Z. Fodor, C. Hoelbling, S. D. Katz, S. Krieg, T. Kurth, L. Lellouch, T. Lippert, K. K. Szabó, and G. Vulvert, J. High Energy Phys. 08 (2011) 148.

[15] C. Allton *et al.* (RBC-UKQCD Collaboration), Phys. Rev. D **78**, 114509 (2008).

[16] Y. Aoki *et al.* (RBC Collaboration, UKQCD Collaboration), Phys. Rev. D **83**, 074508 (2011).

[17] S. N. Syritsyn, J. D. Bratt, M. F. Lin, H. B. Meyer, J. W. Negele *et al.*, Phys. Rev. D **81**, 034507 (2010).

[18] Y. Aoki, T. Blum, H.-W. Lin, S. Ohta, S. Sasaki, R. Tweedie, J. Zanotti, and T. Yamazaki, Phys. Rev. D **82**, 014501 (2010).

[19] J. D. Bratt *et al.* (LHPC Collaboration), Phys. Rev. D **82**, 094502 (2010).

[20] P. Hägler *et al.* (LHPC Collaboration), Phys. Rev. D **77**, 094502 (2008).

[21] C. W. Bernard, T. Burch, K. Orginos, D. Toussaint, T. A. DeGrand, C. DeTar, S. Datta, S. Gottlieb, U. Heller, and R. Sugar, Phys. Rev. D **64**, 054506 (2001).

[22] B. Bistrović, Ph.D. thesis, MIT, 2005.

[23] G. Colangelo, S. Dürr, A. Jüttner, L. Lellouch, H. Leutwyler *et al.*, Eur. Phys. J. C **71**, 1695 (2011).
[24] A. Bazavov *et al.* (MILC Collaboration), Proc. Sci. CD09 (2009) 007.
[25] A. Bazavov, C. Bernard, C. DeTar, X. Du, W. Freeman *et al.*, Proc. Sci. LATTICE2010 (2010) 083.
[26] C. McNeile, C. Davies, E. Follana, K. Hornbostel, and G. Lepage, Phys. Rev. D **82**, 034512 (2010).
[27] S. Dürr, Z. Fodor, C. Hoelbling, S. Katz, S. Krieg, T. Kurth, L. Lellouch, T. Lippert, K. K. Szabo, and G. Vulvert, Phys. Lett. B **701**, 265 (2011).
[28] A. Walker-Loud, H.-W. Lin, D. Richards, R. Edwards, M. Engelhardt *et al.*, Phys. Rev. D **79**, 054502 (2009).
[29] G. Martinelli, C. Pittori, C. T. Sachrajda, M. Testa, and A. Vladikas, Nucl. Phys. **B445**, 81 (1995).
[30] J. A. Gracey, Nucl. Phys. **B662**, 247 (2003).
[31] B. C. Tiburzi and A. Walker-Loud, Nucl. Phys. **A764**, 274 (2006).
[32] W. Detmold, W. Melnitchouk, and A. W. Thomas, Phys. Rev. D **66**, 054501 (2002).
[33] R. G. Edwards and B. Joó (SciDAC, LHPC, and UKQCD Collaborations), Nucl. Phys. B, Proc. Suppl. **140**, 832 (2005).